THE ASTROPHYSICAL JOURNAL, 240:169–179, 1980 August 15

THE SPECTRUM VARIATIONS OF HD 153919

G. G. FAHLMAN[1] AND G. A. H. WALKER[1]
Department of Geophysics and Astronomy, University of British Columbia, Vancouver
Received 1979 September 4; accepted 1980 February 22

ABSTRACT

New spectroscopic observations of the Of star HD 153919, the primary in the 4U 1700−37 X-ray binary system, in the wavelength range 5600–6800 Å, are discussed. The phase-dependent absorption components present in the Hα and the He I λ5876 lines indicate the presence of a gas stream in the stellar wind of the primary. We suggest that the gas stream originates at the inner Lagrangian point of the binary system. The published X-ray photometry is used in conjunction with our spectroscopy to construct a geometrical model of the system which includes a radially symmetric wind from the primary, a heated zone around the secondary, a small coronal region around the primary, and the gas stream. The mass-loss rate from the stellar wind is found to be $6.3 \times 10^{-6}\ M_{\odot}\ \mathrm{yr}^{-1}$ with the stream adding only about 4%.

A series of 27 successive spectra obtained over a 95 minute time interval at a phase during X-ray source eclipse is also discussed. No evidence for rapid variations is found with our noise limit being $\Delta I/I = 0.5\%$. This result indicates that the stellar wind is homogeneous over scales larger than a few times 10^{10} cm.

Subject headings: stars: individual — stars: Of-type — stars: spectrum variables — stars: winds — X-rays: binaries

I. INTRODUCTION

The extreme Of star HD 153919 is the primary component of the eclipsing X-ray source 4U 1700−37 (Jones *et al.* 1973; Penny *et al.* 1973; Hutchings *et al.* 1973). Although the mass function of the system is poorly known (Bahcall 1978), the secondary is probably a neutron star. It moves supersonically through the dense stellar wind of the primary and can be regarded as a probe of the local wind conditions at its orbital distance. Thus the system is of considerable interest in the study of stellar winds from early-type stars.

The secondary does, of course, disturb the stellar wind through its radiation and gravitational fields. The recent *IUE* observations (Dupree *et al.* 1978) show that the resonance lines of C IV, N V, and Si IV do not vary strongly with phase, and hence the effects of X-ray heating as discussed by Hatchett and McCray (1977) must be confined to a small region around the secondary. The gravitational perturbation is expected to lead to a wake trailing the secondary, but it seems highly unlikely that such a wake would be at all detectable in the wind (Carlberg 1978). Thus the secondary is not expected to greatly modify the wind, and any observable effects should be confined closely to phases near 0.5. (All phases discussed here will be based on phase 0.0 corresponding to mid–X-ray–eclipse.)

There are, however, a number of recent observational studies which indicate that the stellar wind is rather strongly affected by the passage of the secondary:

1. Spectroscopy at optical wavelengths (Conti and Cowley 1975; Dachs 1976; Fahlman, Carlberg, and Walker 1977) indicates the presence of a density disturbance in the wind responsible for a distinct blue-shifted absorption component seen in the He I λ5876 and Hα emission lines at phases between approximately 0.6 and 1.0.

2. The broad-band optical photometry by van Genderen (1977) and van Paradijs, Hammerschlag-Hensberge, and Zuiderwijk (1978) shows anomalies which are not easily interpreted. Van Paradijs *et al.* found a period of $3^{d}.41117$ for the system, consistent with the concurrent spectroscopic study of Hammerschlag-Hensberge (1978) and obtain a light curve with the primary minimum occurring at about phase 0.56. Their light curve, however, is not consistent with the variation predicted for a tidally distorted corotating primary. This point is further discussed by Hutchings (1978) who obtains a better match to the shape of the light curve, although the phase shift remains problematical. On the other hand, van Genderen (1977) obtains a period of $3^{d}.4118$, identical to the most recent X-ray period (Branduardi, Mason, and Sanford 1978). He suggests that the deepest light minimum, which, with his ephemeris, occurs at phase 0.63, is due to obscuration by dense gas streams.

3. The narrow-band photometry of Moffat and

[1] Visiting Astronomer, Kitt Peak National Observatory, which is operated by the Association of Universities for Research in Astronomy, Inc., under contract with the National Science Foundation.

Dachs (1977) shows an anomalous increase in the Balmer continuum intensity at a phase between 0.6 and 0.7 depending somewhat on the adopted ephemeris. They suggest that one may be looking down a gas stream which makes approximately a 45° angle with the line connecting the two stars.

4. The 1975 and 1976 *Copernicus* X-ray photometry (Branduardi, Mason, and Sanford 1978) confirms the asymmetrical rise of the hardness ratio (high-energy flux/low-energy flux) just prior to eclipse seen in the 1974 observations (Mason, Branduardi, and Sanford 1976). This phenomenon is consistent with a variable low-energy absorption column along the line of sight to the X-ray source.

In this paper, we present new spectroscopic observations in the wavelength range 5550–6900 Å, which provide further information on the spectroscopic anomalies discussed earlier. A geometrical model of the system is constructed, and we will show that certain features of our data, the X-ray photometry, and perhaps the optical photometry can be understood, at least qualitatively, if the primary is losing a small amount of mass through the inner Lagrangian point of the binary system. In addition, we will discuss a series of 27 spectra obtained over a continuous interval of 95 minutes. These data allow us to place constraints on the scale of any inhomogeneities in the wind.

II. OBSERVATIONS

Our spectra were obtained with the 0.9 m and 2.1 m telescopes at KPNO using the white spectrograph and a 1024 element Reticon linear array of silicon diodes as the detector (Buchholz *et al.* 1976; Walker *et al.* 1977). The mean sample spacing for the spectra was 1.37 Å per diode, with a resolution of about 2 Å. The observations are described in Table 1. In comparing these observations with our earlier data (Fahlman, Carlberg, and Walker 1977), we note that an improvement in the detector cooling system decreased the dark current rate to a negligible level and hence allowed longer integration times. The individual records listed were averaged together to produce the spectra discussed in § III of this paper. The time series (F155/6) is discussed in § IV.

The spectra were low pass filtered to 40% of the Nyquist frequency, divided by a lamp spectrum to remove diode-to-diode sensitivity variations and then rectified by fitting low-order polynomials through selected continuum points. The wavelength scale was established by dispersion curves derived for He-Ne-Ar lamp spectra obtained before and after each exposure. Although the dispersion curves can be very accurately determined, the zero point of the wavelength scale is not well known because of slight shifts of the spectra relative to the diode array. The scale adopted here is such that the weighted average velocity of the λ5780, D1, D2 sodium lines and the λ6614 interstellar lines is zero.

We emphasize here that the phases listed in Table 1 are based on the recent X-ray ephemeris of Branduardi, Mason, and Sanford (1978). These parameters give phases which are 0.13 later than those computed with the ephemeris of Hutchings (1974), which has been used extensively in the past. The ephemeris of van Paradijs, Hammerschlag-Hensberge, and Zuiderwijk (1978) and Hammerschlag-Hensberge (1978) gives phases which are 0.08 earlier than those listed. In computing phases, we have assumed a circular orbit, but it should be noted that an apparently significant eccentricity of $e = 0.19$ was found by Hammerschlag-Hensberge (1978), whereas Hutchings (1978) used a value of $e = 0.05$ in his light-curve solutions. Our view is that the X-ray period is probably the most reliable, since it is based on the longest time interval, and that the question of whether the orbit is circular is still open. A small eccentricity, however, would not significantly affect the following discussion.

III. THE PHASE-DEPENDENT VARIATIONS

The spectra at the five phases listed in Table 1 are plotted in Figure 1 in two segments around He I λ5876 and Hα. The radial velocities of a few selected lines are listed on Table 2. Also included are similar data from our 1976 observations where the phase of that data has been recomputed for the ephemeris adopted here. The measurement errors are very small (± 5 km s^{-1} at most), but the systematic effects caused by the

TABLE 1

SPECTROSCOPIC OBSERVATIONS

Data File	JD[a] (2,442,000)	Phase[b]	Exposure Time[c] (seconds)	Number of Records	Telescope
F57/59	3677.782	0.043	1200	3	0.9
F88	3678.767	0.332	1800	2	0.9
F124	3679.783	0.630	1200	4	0.9
F155	...	...	100	8	2.1
F156	3680.779	0.922	200	25	2.1
F197	3681.767	0.212	1200	1	2.1

[a] Midexposure of all records.

[b] Phase computed with $P = 3^d.4118$, $T_0 = 2442476^d.68$.

[c] For a single record.

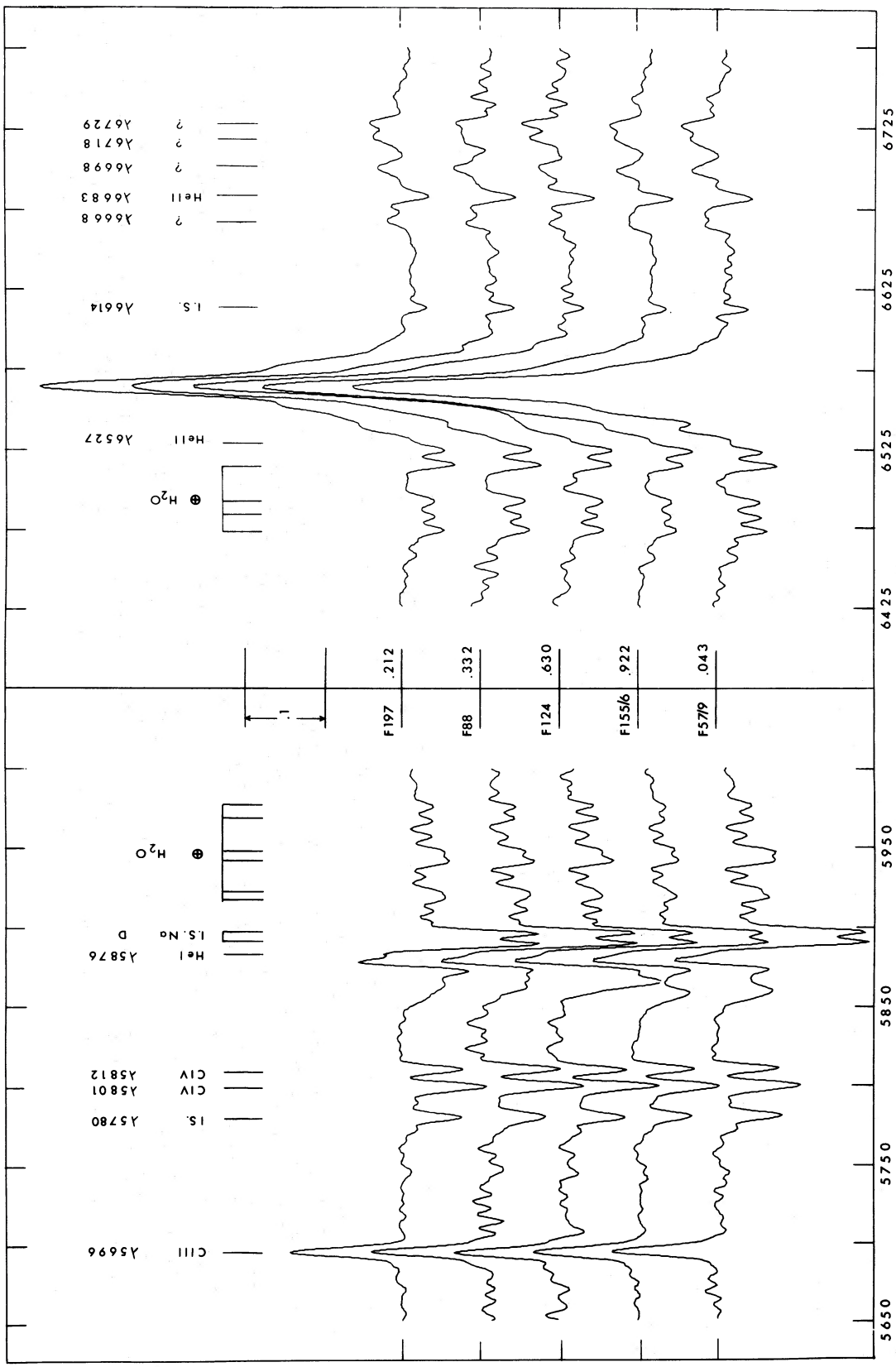

FIG. 1.—Mean, filtered, and rectified spectra are shown in the 2 spectral regions near He I λ5876 (*left*) and Hα (*right*)

TABLE 2

RADIAL VELOCITIES OF SELECTED LINES (km s^{-1})

		Emission Peak				Absorption Minimum	
Year	Phase	C IV λ5696	He I λ5876	Hα λ6563	C IV λ5801	C IV λ5812.1	He II λ6406.3
1978	0.043	−47	171	90	−116	−84	−30
1978	0.212	−15	152	84	−94	−83	−29
1978	0.322	−26	176	106	−80	−75	−12
1978	0.630	−69	177	84	−89	−111	−59
1978	0.922	−63	174	70	−117	−92	−54
1976	0.007	−105	160	78	−118	−91	−36
1976	0.403	−87	230	88	−120	−113	−9
1976	0.706	−101	189	70	−111	−93	−92
1976	0.821	−95	155	53	−136	−126	−60

spectral shifts discussed above limit the accuracy of these velocities to about ±20 km s^{-1}.

In comparing our two sets of data and also the results of Conti and Cowley (1975), we see that the Hα and He I λ5876 emission peaks show erratic shifts of about 50 km s^{-1}, but there are no obvious systematic changes with epoch. However, the C III λ5696 line apparently suffered a systematic change with the 1978 data having a lower velocity. The C IV λ5801, λ5812 absorption lines seem to show a smaller, but still noticeable, change. A similar variation with epoch of the velocities of these lines has also been noted by Conti and Cowley (1975). Such effects are indicative of long time-scale changes in the stellar wind. The He II λ6406 absorption line velocities follow only very roughly the velocity curve of the primary which appears typical of single line velocities (cf. Hutchings 1974; Hammerschlag-Hensberge 1978).

An interesting spectral feature seen in Figure 1 is the weak emission-line complex on either side of the He II λ6683 absorption line. The continuum level in this region is difficult to establish, but the reality of the features has been checked by dividing the HD 153919 data by spectra of the O7.5 star HR 6781 which were also obtained on each night. The lines at λ6668 and λ6698 appear in other extreme Of stars and have been tentatively identified with [Ni II] and [Fe II], respectively (Hutchings 1979). The λ6668.8 of [Ni II] is present in the spectrum of η Car (Thackeray 1967), and its identification in HD 153919 seems reasonable. The identification of λ6698 with [Fe II] is less plausible. In view of the transition probabilities computed by Garstang (1962), an identification with the λ6698.02 line of the multiplet 32*F* is highly unlikely. The λ6700.7 transition of multiplet 43*F* is a more promising possibility; but this line, the weakest in the multiplet, was not detected in the rich [Fe II] spectrum of η Car (Thackeray 1967). The two lines appearing in our spectra at λ6718 and λ6729 have, to our knowledge, not been noted previously. They coincide very nicely with the [S II] doublet. The λ6629.86 transition of the [Fe II] muultiplet 31*F* may also be involved here. Although not shown in Figure 1, previously reported emission lines at λ6217 and λ6396 are weakly present in our spectra. The former is unidentified. The latter is suggested to be an [Fe II] transition, apparently belonging to multiplet 44*F*. This identification is suspect because the strongest member of that particular multiplet, at λ6188.55, is not seen. Perhaps the only definite statement one can make here is that weak emission lines of uncertain origin are present throughout the spectra not only of HD 153919, but in those of other extreme Of stars as well. For that reason they seem worthy of further study at higher dispersion.

To see the orbital variations more clearly, we have adopted F197 ($\phi = 0.23$) as a reference and subtracted it from the spectra at the other phases as shown in Figure 2. This figure should be compared to a similar plot in Fahlman, Carlberg, and Walker (1977). The anomalous blueshifted absorption in the He I λ5876 profile is clearly visible in the Hα region as well. Indeed the differences at Hα and He I λ5876 match very well and support our earlier result that a large-scale density disturbance in the wind is visible against the primary at phases from about 0.6 to somewhat beyond mid-eclipse of the X-ray source and is moving outward from the primary at about 800 km s^{-1}.

The interesting new result seen in the present data is the exceptionally strong absorption at the phase 0.630. Its velocity is −500 km s^{-1}, significantly greater than the −800 km s^{-1} typical of the anomalous component at phases 0.922 and 0.043 and significantly lower than the −200 km s^{-1} of the ordinary P Cygni absorption. The observation is of interest because: (1) the photometric anomalies described by van Genderen (1977) and by Moffat and Dachs (1977) also occur at this phase, and (2) there is no firm evidence for spectroscopic anomalies to appear prior to this phase. If we interpret the spectroscopic anomalies as being due to a gas stream, the implication is that we are looking down at the origin of the stream at phase 0.63.

For three reasons, the stream is almost certainly not a wake associated with the secondary: (1) If we adopt Hutchings's (1976) values for the orbital velocity of 400 ± 70 km s^{-1} and assume that the wind rotational

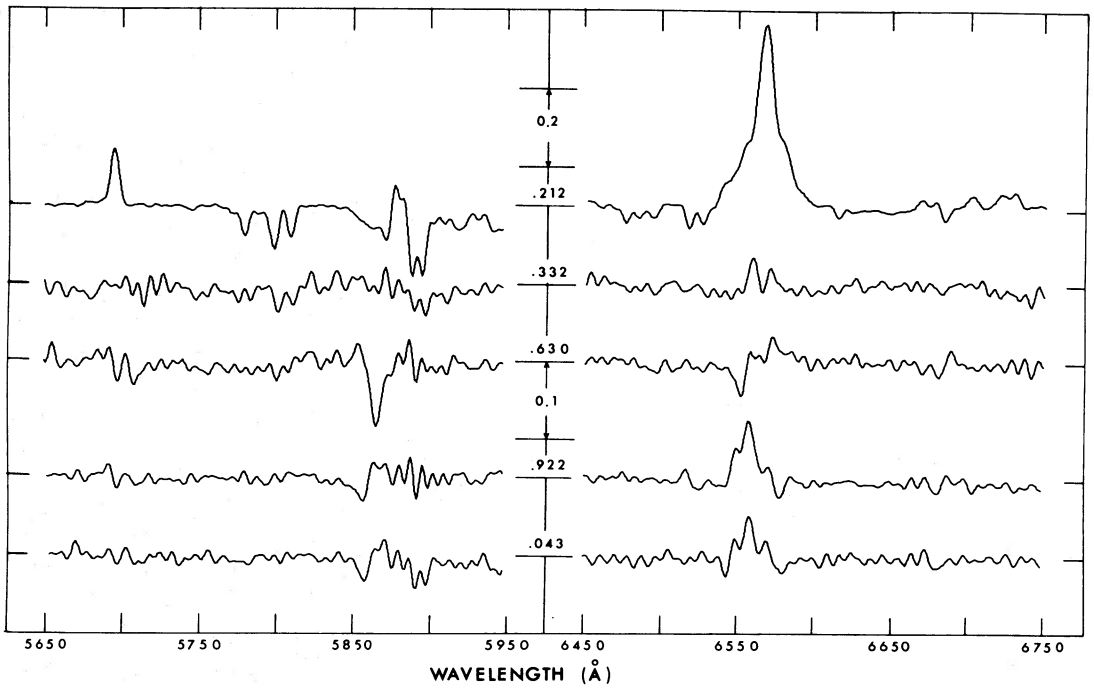

FIG. 2.—The differences (FX − F197) are shown below the F197 spectrum. This figures shows that the variable absorption feature easily seen in the He I λ5876 line is also present at Hα. The variations at the C IV emission line and the He II absorption line are due to radial velocity variations.

speed is determined by the conservation of angular momentum as it leaves the synchronously rotating primary, the observed wind velocity of -500 km s^{-1} leads to a wake pointing back at $21° \pm 7°$, rather than the observed 45°. (2) The X-ray photometry does not show a noticeable absorption feature at phase 0.63. (3) The wake has a characteristic dimension given by the accretion radius of the secondary ($\sim 10^{10}$ cm) and could not cause any appreciable obscuration of the primary (Carlberg 1978).

With respect to point (1) above, we note that there is some question whether the primary star is rotating synchronously or not (cf. Hutchings 1976; Conti 1978). If the primary is rotating at about one-half the synchronous rate (as indicated by the absorption lines), the wake angle estimated above is increased to $31° \pm 6°$. To obtain a wake angle of 45°, it is also necessary to reduce the radial velocity of the wind at the orbit of the X-ray source to ~ 300 km s^{-1}. This, however, is inconsistent with the radial velocity of the absorption features to be explained by the wake. Moreover, points (2) and (3) above must still be addressed. In our view, the arguments supporting synchronism are more compelling, but, in any case, the wake is unlikely to be a significant factor in explaining the observational data.

The next most likely source of the gas stream is mass loss through the inner Lagrangian point of the binary system. The primary is probably just within its critical Roche lobe (Hutchings 1978) so that catastrophic mass loss does not occur. It will be argued below that only a modest density enhancement flowing from the critical point is suggested by the observational data.

A drawing illustrating the structure we propose for the stellar wind is shown in Figure 3 together with the He I λ5876 profiles observed with our Reticon system. The parameters adopted to draw this diagram are summarized in Table 3. The wind velocity must be about 500 km s^{-1} close to the stellar surface, and we assume that the wind is quickly accelerated as it leaves the stellar surface and reaches a plateau velocity of 800 km s^{-1} by the time it arrives at the X-ray source. We associate the disappearance of the anomalous absorption profile with a region of rapid acceleration up to the terminal velocity of 2600 km s^{-1} (Dupree *et al.* 1978) which occurs at about 8 R_*. The velocity law is similar in form (but different in scale) to that adopted by Cassinelli, Olsen, and Stalio (1978) in their discussion of the wind from ζ Ori.

Two features of the diagram are the X-ray–heated zone surrounding the secondary (Hatchett and McCray 1977) and a high-temperature corona extending to 1.2 R_* around the primary (cf. Cassinelli, Olsen, and Stalio 1978). The existence of these regions is suggested by attributing the observed phase-dependent X-ray hardness ratio (Mason, Branduardi, and Sanford 1976; Branduardi, Mason, and Sanford 1978) to a variable low-energy absorption column seen in front of the X-ray source.

The outer boundary of the hot zone drawn around the secondary corresponds to the radius where $n(O^{+7})/n(O) = 0.1$, and the gas within this zone should be fully transparent to X-rays. For the 20

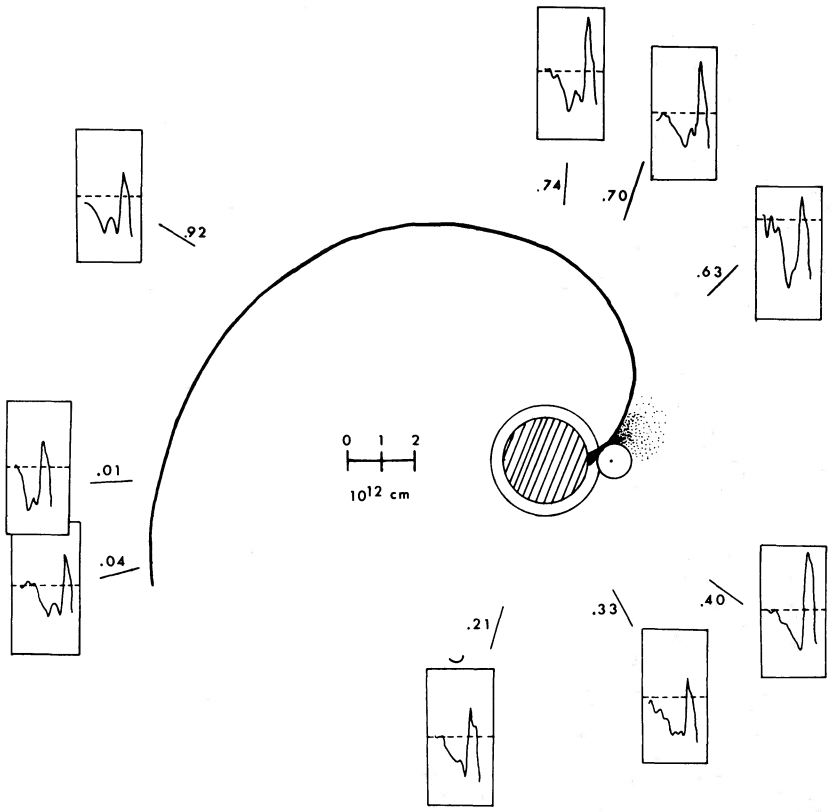

FIG. 3.—The proposed geometrical model of the binary system, as discussed in the text, is shown together with the phase-dependent He I λ5876 profiles observed by us. Each box has a width of 50 Å and a height of $\Delta I = 0.2$, where the intensity is relative to the dashed continuum level. The proposed gas stream leaves the inner Lagrangian point and is deflected behind the hot zone around the secondary by radiation pressure. After leaving the vicinity of the secondary, the stream is expected to follow a trajectory defined by the free stream line drawn as a heavy solid line. It is this gas stream which gives rise to the extra absorption components in the He I λ5876 and Hα lines apparent in Figs. 1 and 2. The X-ray photometry implies the existence of additional material behind the secondary at phases 0.5 to 0.63 as indicated in the figure.

keV bremsstrahlung spectrum adopted here, the corresponding value of log ξ is 2.86, where $\xi = L_x/n_o R_0^2$ and L_x is the X-ray luminosity, n_0 is the density at the orbital radius R_0. For a uniform velocity wind the surfaces of constant ξ are spheres of radius $r_1 = R_0 q^{1/2}/|q - 1|$ centered at a distance $r_2 = R_0/|q - 1|$ from the secondary in the direction away from the primary, where $q = \xi n_0 R_0^2/L_x$. To solve for the density n_0, we adopt a value for the column density behind the X-ray source at phase 0.5 of $N_c(0.5) = 2 \times 10^{23}$ cm^{-2}. This value is estimated from the hardness ratio curve of Mason, Branduardi, and Sanford (1976). Equating this column density to that computed for a uniform velocity wind extending from $R_1 = R + r_1 + r_2$ to $R_2 = \infty$, we find a value of $n_0 = 1.3 \times 10^{11}$ cm^{-3}. The density in turn gives $r_1 = 4.96 \times 10^{11}$ cm and $r_2 = 1.18 \times 10^{11}$ cm with $q = 17.6$. We note here that the mass-loss rate derived from the density and velocity at the X-ray source orbit is $M = 6.3 \times 10^{-6}\, \dot{M}_\odot$ yr^{-1} in good agreement with other estimates (cf. Hutchings 1979).

TABLE 3

ADOPTED SYSTEM PARAMETERS

Parameter	Value
Primary radius (R_*)	1.4×10^{12} cm
Orbital radius (R_0)	2.0×10^{12} cm
Orbital velocity of secondary	400 km s^{-1}
Wind velocity at R_0	800 km s^{-1}
Wind rotation at R_0	200 km s^{-1}
X-ray luminosity (L_*)	2.1×10^{37} ergs s^{-1}
X-ray spectrum upper cutoff energy	20 keV

Neglecting for the moment the stream and coronal region of Figure 3, we use the derived density to compute the column density in front of the X-ray source around the orbit. This is shown as the solid line in Figure 4 with the points being the values observed in 1974 by Mason, Branduardi, and Sanford (1976). We note that the anomalously low value at $\phi = 0.22$ is not seen in the 1975 and 1976 observations (Branduardi, Mason, and Sanford 1978), but the observed asymmetry is certainly a permanent feature, as are the low values (compared to the prediction) at eclipse ingress and egress. If we now include an X-ray transparent coronal region extending around the primary to $R_c = 1.2R_*$ the computed column densities

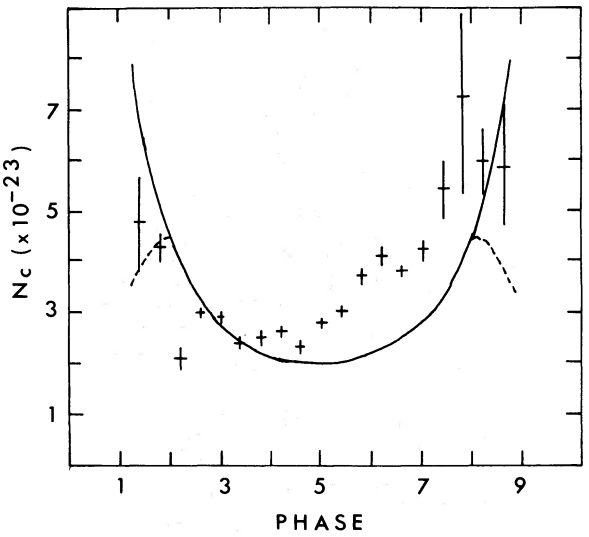

FIG. 4.—The solid line is the column density in front of the X-ray source due to the radially symmetric stellar wind emanating from the primary excluding the hot zone around the secondary. The dashed lines show how the curve is modified when a transparent corona extending to 1.2 R_* surrounds the primary. The points with vertical error bars are the values of the hardness ratio observed by Mason, Branduardi, and Sanford (1976), converted to an equivalent column density under the assumption that the spectral changes are due to absorption. The asymmetry of the observed curve indicates the presence of additional absorbing gas behind the secondary which we interpret to be the gas stream shown in Fig. 3.

do turn down, as shown by the dashed lines in Figure 4, in somewhat better agreement with the observations.

From Figure 4, it can be seen that from about $\phi = 0.6$ to eclipse ingress the departure of the observed curve from the calculated one is consistent with an additional absorption column of about 1.5×10^{23} cm^{-2} in front of the X-ray source. We identify this with the gas stream coming from the inner Lagrangian point. Given a characteristic scale of 0.1 R_* for the stream (cf. Savonije 1979) near its source, its density is estimated to be 1.1×10^{10} cm^{-3} or about 4 times the ambient wind density. The mass loss from the stream is an insignificant 4% of the loss due to the wind. The calculations of Hatchett, Buff, and McCray (1976) indicate that the radiation pressure of the X-rays reaches a maximum at $\log \xi = 2.15$. For the stream density of 1.1×10^{10} cm^{-3}, the surface $\log \xi = 2.15$ very nearly coincides with the $\log \xi = 2.86$ surface in the ambient stellar wind. Consequently it seems quite plausible that the stream is in fact deflected around the trailing edge of the X-ray–heated region as shown in Figure 3. Now the hardness ratio begins to deviate from the "streamless" model at about $\phi = 0.5$, which indicates that there is additional material behind the X-ray–heated sphere. This could be stream material which simply passes through the hot region or material which is evaporated off the side of the stream exposed to the X-ray source. The presence of a slight density excess behind the secondary is also indicated by the increase in the Hα emission at phases near X-ray source passage (Conti and Cowley 1975).

IV. SHORT TIME-SCALE VARIABILITY

Matilisky, La Sala, and Jessen (1978) reported a possible 97 minute periodicity in the 1–10 keV X-ray flux from 4U 1700−37, although a subsequent analysis by Hammerschlag-Hensberge, Henrichs, and Shaham (1979) has certainly cast doubt on the reality of the periodicity. However, recent work by Carlberg (1978, 1979) has shown conclusively that radiatively driven stellar winds, as proposed by Caster, Abbot, and Klein (1975), are subject to instabilities with characteristic growth times of ~1 hr. The wind is expected to break up into blobs as it moves away from the star. There have been persistent reports of rapid spectrum variations in early-type stars (see Lacy 1977 for a detailed summary and critique) but little convincing evidence for such a phenomenon.

We obtained an almost continuous series of spectra of HD 153919 over a 97 minute interval on 1976 June 3 and have examined this data for evidence of rapid variability.

The time series is displayed in Figure 5. From an inspection of the telluric features, small random shifts of typically 0.1 pixel (2.5 μm) were detected between successive spectra. Consequently, it was necessary to align the spectra. This alignment was accomplished by applying the appropriate phase shift to the Fourier transform of the spectra after filtering to 40% of the Nyquist frequency and division by a lamp spectrum. The spectra were not, however, interpolated to a uniform wavelength scale nor were they rectified. It is clear from Figure 5 that none of the spectral features show velocity shifts over the time span of the data. A shift as small as 5 km s^{-1} would be noticeable.

The 27 spectra of Figure 5 were added to produce a mean spectrum. In Figure 6 we show the residuals obtained by subtracting the mean from each spectrum. We note that each of the first four spectra are the sum of two 100 s exposures, whereas the remaining 23 are 200 s exposures, which accounts for the apparent difference in noise amplitude. (There is a 400 s gap between the fourteenth and fifteenth records as a result of unrecoverable tape error which occurred during the run.)

The maximum amplitude in the residuals is about ±5%. The standard deviation about the mean of each difference is shown in Figure 7. This measures the scatter in the horizontal direction in Figure 6 and is a good estimate of the signal-to-noise ratio in the individual spectra. Figure 8 is a plot of the standard deviation per diode (i.e., the vertical variations of Fig. 6) expressed as a percentage of the mean spectrum and smoothed to the same extent as the data itself. The increase in the variance toward the red is an artifact due to a change in the spectral shape caused by differential extinction and refraction as the star reached larger zenith distances toward the end of the run. There is no sign of any significant variations in the He I λ5876 and Hα profiles.

From these results we conclude that the stellar wind

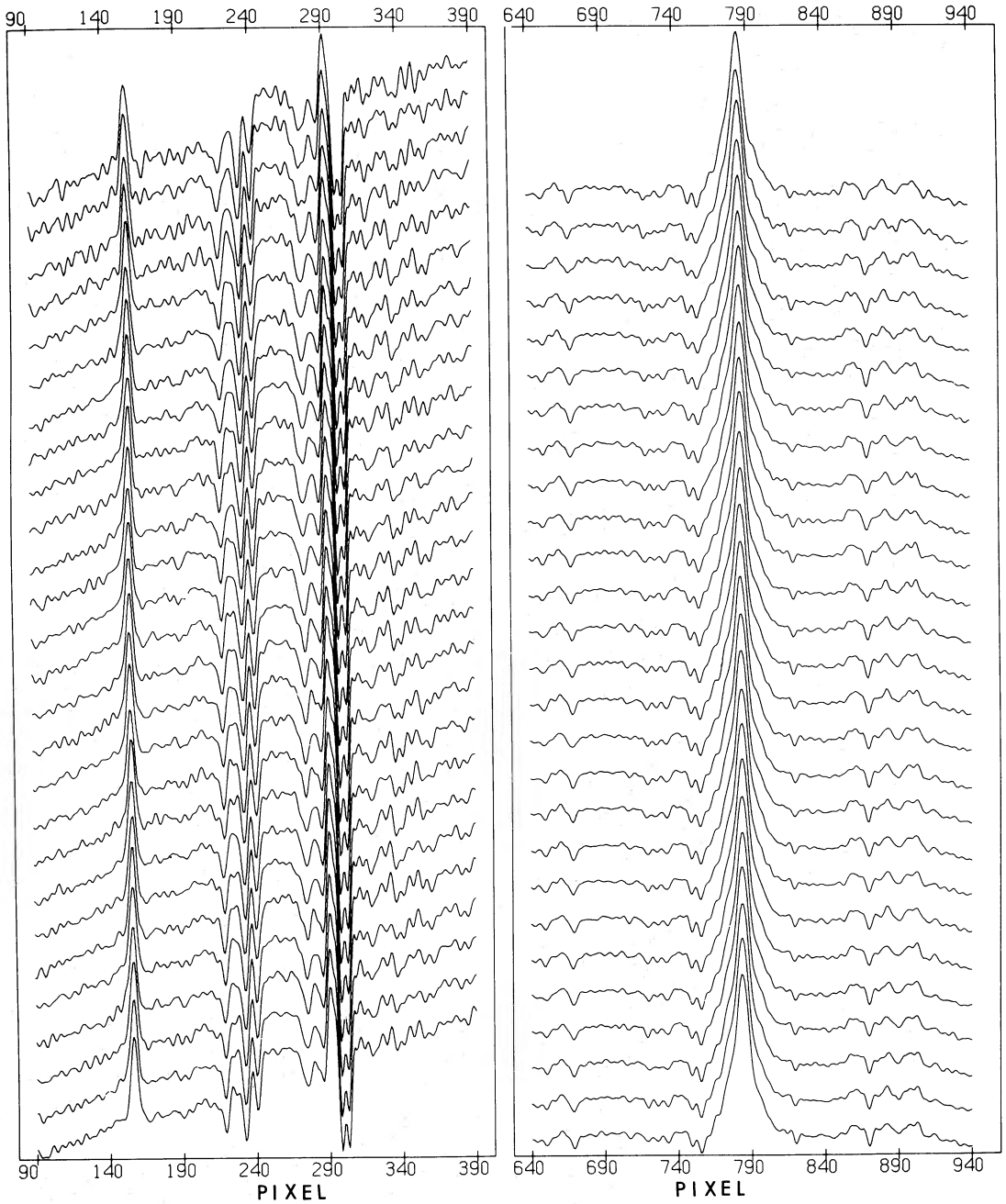

FIG. 5.—The time series of spectra obtained at phase 0.92 is shown in two segments. (Time increases downward.) These spectra were not rectified nor interpolated to a wavelength scale. The corresponding dispersion curve is $\lambda(\text{Å}) = \sum_{i=0}^{3} a_i x^i$, where x is the pixel number and $a_0 = 5482.0761$, $a_1 = 1.3339594$, $a_2 = 1.1225603 \times 10^{-4}$, and $a_3 = -7.0690645 \times 10^{-8}$.

is homogeneous over length scales corresponding to the velocity resolution of our data ($\delta v \approx 130$ km s^{-1}). The thickness of the velocity shell resolved by the data is given approximately as $\delta l \approx \delta v/(dv/dr)$, where the velocity gradient may be estimated as v/r. The volume observed is $r^2 \delta l \approx r^3(\delta v/v) \approx 10^{36}$ cm^3 for $r = 2 \times 10^{12}$ cm and $v = 10^8$ cm s^{-1}. Since any short-term fluctuations are less than 1%, we conclude that if the emission arises from randomly distributed blobs, then there are at least 10^4 such blobs within the sampled volume. The typical size of a blob is then 4×10^{10} cm, a value which is consistent with the stability analysis of Carlberg (1978, 1979).

V. SUMMARY AND DISCUSSION

By adopting the point of view that the X-ray source in this system is acting as a probe of the

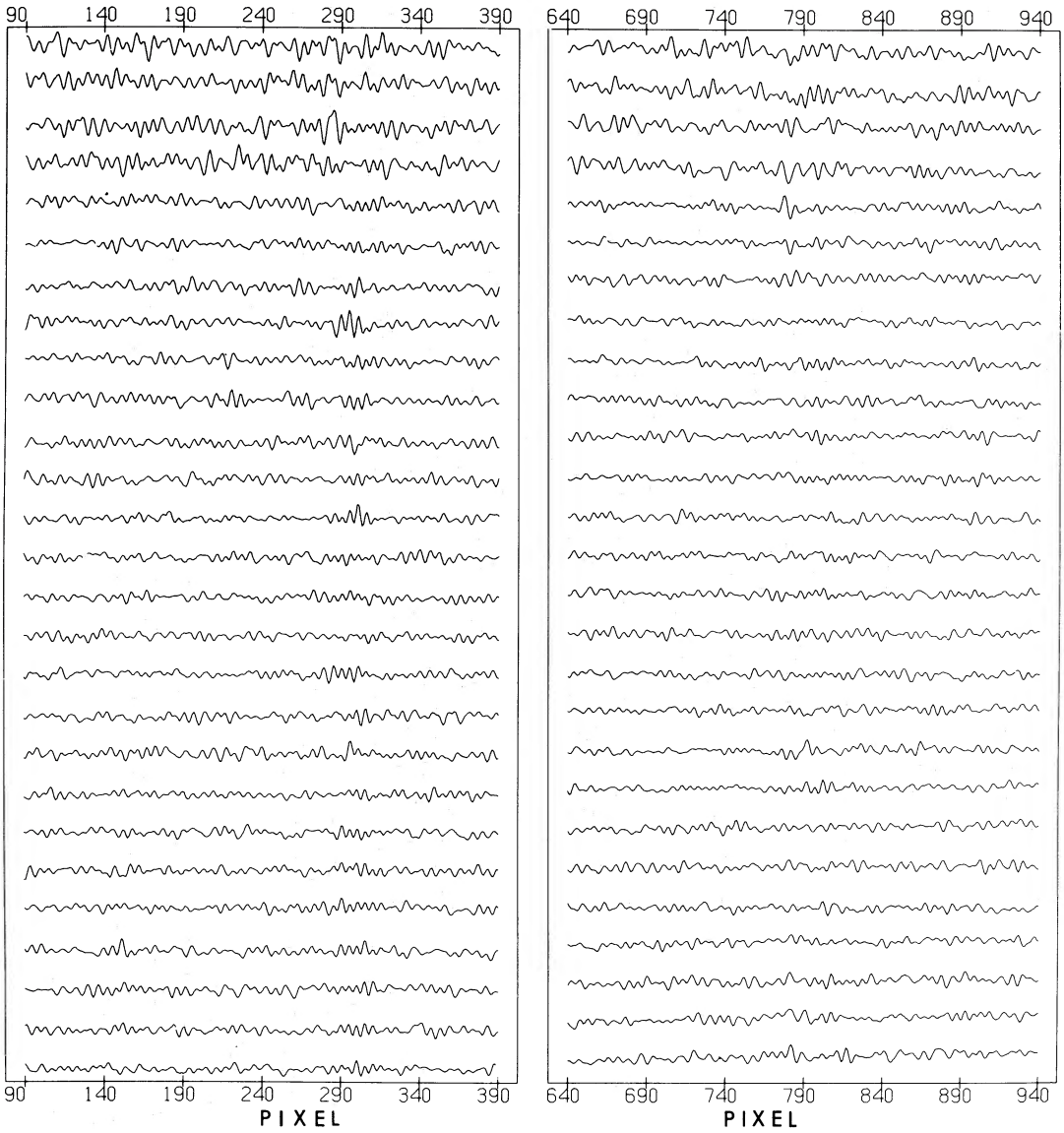

FIG. 6.—The residuals obtained after subtracting the mean spectrum from the individual spectra in Fig. 5. This plot is a convincing demonstration of the lack of any significant variability in the spectrum.

stellar wind, we have shown how the *Copernicus* observations, in conjunction with the optical observations, can be used to obtain information about the density structure of the wind. Four components which contibute to the observed phenomena have been identified: (1) an underlying radially symmetric wind which has a density of 1.3×10^{11} cm^{-3} at the orbit of the X-ray source and velocity profile consisting of a region of rapid initial acceleration to about 800 km s^{-1} and a second region of acceleration beyond about 8 R_* to the terminal velocity of 2600 km s^{-1}; (2) a zone of gas around the secondary heated by its X-ray flux; (3) a coronal zone extending to about 1.2 R_* around the primary; and (4) a stream of matter with a density of about 4 times the ambient density leaving the inner Lagrangian point and deflected behind the secondary by radiation pressure from the X-rays.

The hot zone around the secondary is postulated mainly on the basis of the theoretical calculations of Hatchett and McCray (1977). If this zone is entirely absent, the density at the orbit of the secondary, as estimated from the hardness ratio, is decreased by about 30%, but the functional shape of the calculated column density in front of the X-ray source is also changed, leading to a somewhat poorer match to the observations than is indicated by Figure 4.

The existence of the coronal region around the primary is suggested solely by the dip in the hardness ratio near the eclipse ingress and egress points. Small coronal regions around early-type stars have been suggested previously to explain the ionic structure ob-

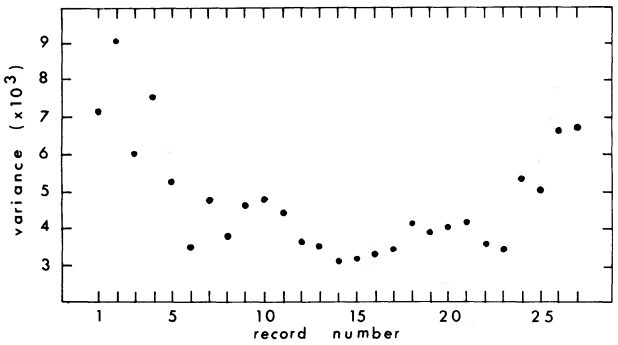

FIG. 7.—The variance in each residual spectrum of Fig. 6 is plotted. (The calculation includes the entire 1024 pixels of each spectrum.) The first 4 records are the sum of 2 100 s exposures and are expected to have $\sqrt{2}$ more noise than the remaining 200 s exposure records. The variances of the last 4 records are high, primarily because of a slight uncompensated trend in the reddest end of the residuals.

served in the ultraviolet (Olsen 1978) and to match the Hα emission profiles seen in ζ Ori (Hearne 1975) and ζ Pup (Cassinelli *et al.* 1978). Obviously the observed Hα profiles from HD 153919 should be modeled to provide confirmation and perhaps further information on the properties of the postulated coronal region. The only property we have assumed is that the coronal region be transparent to the X-ray flux from the secondary. In particular, we have not made any allowance for the fact that such a region would be a source of soft X-rays and would modify the ionic structure of the wind. Thus our density estimate would be a lower limit, because the wind would not be a completely cold absorption column in front of the X-ray source.

Finally, the stream has been proposed to explain the asymmetry in the column density of matter seen in front of the X-ray source. As the stream leaves the vicinity of the secondary, it will be carried out into the wind giving rise to the blueshifted absorption components seen at Hα and He I λ5876. The initial part of the stream may also account for the photometric anomalies discussed in the introduction.

The mass-loss rate from the stellar wind is found to be $6.3 \times 10^{-6}\ M_{\odot}\ \mathrm{yr}^{-1}$. For a terminal velocity of $v_{\infty} = 2600\ \mathrm{km\ s}^{-1}$, the theory of Wright and Barlow (1975) predicts a 3 cm radio flux of 1.4 mJy, if the distance to the system is 1.7 kpc (Bolton and Herbst 1976). Since the terminal velocity is known with some certainty, a radio flux measurement (which is sensitive to the outermost regions of the expanding envelope) would provide an important check on the mass-loss rate and hence the wind density. Any free-free infrared emission, however, originates much closer to the photosphere and thus could provide valuable information on the velocity law in the wind.

A basic point of uncertainty arises in our intepretation because of the conflicting claims for the period of the system and the epoch of mid–X-ray–eclipse which, of course, affects the phasing of the phenomena seen around the orbit. Our model, which depends heavily on the anomalies seen near phase 0.63 with the *Copernicus* ephemeris, would still be feasible if the ephemeris of Hammerschlag-Hensberge (1978) is adopted, but would require that the stream be more strongly influenced by the X-rays. In particular the deflection angle of the stream would be closer to 70° than 45°, and the observations would then require a

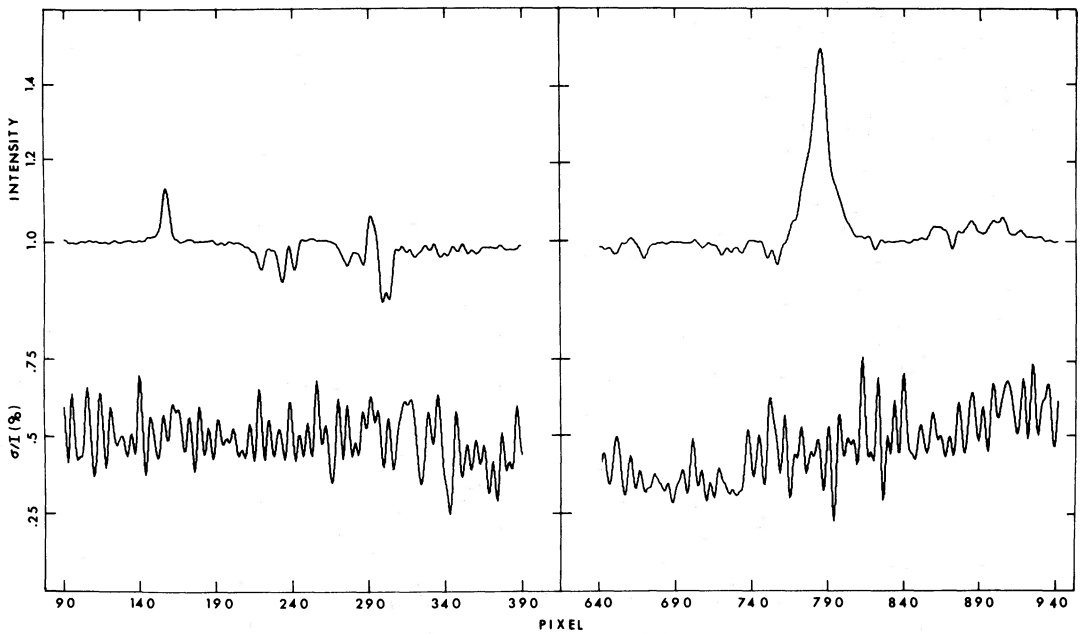

FIG. 8.—The variance, σ, of each pixel, expressed as a percentage of the intensity, *I*, in the mean rectified spectrum, is plotted below the mean spectrum. The trend apparent to the right of Hα is due to differential atmospheric extinction. This figure shows the magnitude of the vertical variation in Fig. 6, whereas Fig. 7 displays the horizontal variation. Evidently the mean variance in both directions is the same, indicating that the time variations are simply due to the noise in each spectrum.

higher degree of "backfilling" behind the X-ray source.

A second point is that the X-ray luminosity is highly variable on a time scale of ~ 1 hr. The extent of the heated zone around the secondary and the location of the stream will vary in response to these changes. Therefore at the critical phase of 0.63, variations in the absorption profiles of Hα and He I λ5876 may be detectable over hourly time scales. Our data, which consists of four 20 minute exposures at this phase, shows no convincing evidence for variability. The X-ray hardness ratio certainly changes from cycle to cycle, and we expect the optical line profiles to change as well over this time scale. In particular, the orientation angle of the stream may be different on successive cycles which would tend to blur the phase dependence of the associated optical phenomena.

The ultimate source of the variability is most likely the small-scale inhomogeneity arising from the inherent instability of the radiatively driven wind (Carlberg 1978). Our low-resolution observations of the optical emission lines sample isovelocity surfaces which enclose rather large volumes in the wind and hence are insensitive to the small-scale structure predicted.

Nevertheless, the data discussed in § IV places a fairly restrictive limit on the degree of inhomogeneity in the wind. The scale lengths involved cannot be much greater than 10^{10} cm if the wind is imagined to consist of randomly distributed blobs. The high degree of X-ray variability is, however, consistent with the concept of a chaotic, inhomogeneous wind over small length scales. It would be very desirable to obtain a series of high-resolution spectra of Hα over a time span of a few hourse in order to better quantify the degree of inhomogeneity in the wind.

We thank Stephenson Yang for his assistance in the data reduction and Ray Carlberg for his comments on the rapid variability. This work was supported through operating grants from the National Science and Engineering Research Council of Canada.

REFERENCES

Bahcall, J. N. 1978, *Ann. Rev. Astr. Ap.*, **16**, 241.
Bolton, C. T., and Herbst, W. 1976, *A.J.*, **81**, 339.
Branduardi, G., Mason, K. O., and Sanford, P. W. 1978, *M.N.R.A.S.*, **185**, 137.
Buchholz, V. L., Walker, G. A. H., Glaspey, J. W., Isherwood, B. C., and Lane-Wright, D. 1976, *Adv. Electronics Electron. Phys.*, **40B**, 879.
Carlberg, R. G. 1978, Ph.D. thesis, University of British Columbia.
———. 1979, *J.R.A.S. Canada*, **73**, 299.
Cassinelli, J. P., Olsen, G. L., and Stalio, R. 1978, *Ap. J.*, **220**, 573.
Castor, J. I., Abbott, D. C., and Klein, R. I. 1975, *Ap. J.*, **195**, 157.
Conti, P. S. 1978, *Astr. Ap.*, **63**, 225.
Conti, P. S., and Cowley, A. P. 1975, *Ap. J.*, **200**, 133.
Dachs, J. 1976, *Astr. Ap.*, **47**, 19.
Dupree, A. K. *et al.* 1978, *Nature*, **275**, 400.
Fahlman, G. G., Carlberg, R. G., and Walker, G. A. H. 1977, *Ap. J. (Letters)*, **217**, L35.
Garstang, R. H. 1962, *M.N.R.A.S.*, **124**, 321.
Hammerschlag-Hensberge, G. 1978, *Astr. Ap.*, **64**, 399.
Hammerschlag-Hensberge, G., Henrichs, H. F., and Shaham, J. 1979, *Ap. J. (Letters)*, **228**, L75.
Hatchett, S., Buff, J., and McCray, R. 1976, *Ap. J.*, **206**, 847.
Hatchett, S., and McCray, R. 1977, *Ap. J.*, **211**, 552.
Hearne, A. G. 1975, *Astr. Ap.*, **40**, 277.
Hutchings, J. B. 1974, *Ap. J.*, **192**, 677.
———. 1976, in *X-ray Binaries*, ed. E. Boldt and Y. Kondo (NASA SP-389), p. 531.
Hutchings, J. B. 1978, *Ap. J.*, **226**, 264.
———. 1979, *Pub. A.S.P.*, in press.
Hutchings, J. B., Thackeray, A. D., Webster, B. L., and Andrews, P. J. 1973, *M.N.R.A.S.*, **163**, 13P.
Jones, C., Forman, W., Tananbaum, H., Schreier, B., Gursky, H., and Kellogg, L. 1973, *Ap. J. (Letters)*, **181**, L43.
Lacy, C. H. 1977, *Ap. J.*, **212**, 132.
Mason, K. O., Branduardi, G., and Sanford, P. 1976, *Ap. J. (Letters)*, **203**, L29.
Matilisky, T., La Sala, J., and Jessen, J. 1978, *Ap. J. (Letters)*, **224**, L119.
Moffat, A. F. J., and Dachs, J. 1977, *Astr. Ap.*, **58**, L5.
Olsen, G. L. 1978, *Ap. J.*, **226**, 124.
Penny, A. J., Olowin, R. P., Penfold, J. E., and Warren, P. R. 1973, *M.N.R.A.S.*, **163**, 7P.
Savonije, G. J. 1979, *Astr. Ap.*, **71**, 352.
Thackeray, A. D. 1967, *M.N.R.A.S.*, **135**, 51.
van Genderen, A. M. 1977, *Astr. Ap.*, **54**, 683.
van Paradijs, J. A., Hammerschlag-Hensberge, G., and Zuiderwijk, E. J. 1978, *Astr. Ap. Suppl.*, **31**, 189.
Walker, G. A. H., Buchholz, V. L., Fahlman, G. G., Glaspey, J., Lane-Wright, D., Mochnacki, S., and Condal, A. 1977, *IAU Colloquium 40, Astronomical Applications of Image Detectors with Linear Response*, ed. M. Duchesne and G. Lelievre (Meudon: Obs. Paris).
Wright, A. E., and Barlow, M. J. 1975, *M.N.R.A.S.*, **170**, 41.

G. G. FAHLMAN and G. A. H. WALKER: Department of Geophysics and Astronomy, University of British Columbia, 2075 Wesbrook Mall, Vancouver, B.C. V6T 1W5, Canada